

PRaFULL: A method for the analysis of piled raft foundation under lateral load

Stefano Stacul^{*1}, Nunziante Squeglia¹ and Gianpiero Russo²

¹Department of Civil and Industrial Engineering, University of Pisa, Largo Lucio Lazzarino 1, 56122, Pisa, Italy

²Department of Civil, Architectural and Environmental Engineering, University of Naples Federico II, Via Claudio 21, 80125, Naples, Italy

(Received September 27, 2019, Revised February 7, 2020, Accepted February 12, 2020)

Abstract. A new code, called PRaFULL (Piled Raft Foundation Under Lateral Load), was developed for the analysis of laterally loaded Combined Pile Raft Foundation (CPRF). The proposed code considers the contribution offered by the raft-soil contact and the interactions between all the CPRF system components. The nonlinear behaviour of the reinforced concrete pile and the soil are accounted. As shallower soil layers are of great relevance in the lateral response of a pile foundation, PRaFULL includes the possibility to consider layered soil profiles with appropriate properties. The shadowing effect on the ultimate soil pressure is accounted, when dealing with pile groups, as proposed by the Strain Wedge Model. PRaFULL BEM code obviously requires less computational resources compared to FEM (Finite Element Method) or FDM (Finite Difference Method) codes. The proposed code was validated in the linear elastic range by comparisons with the code APRAF (Analysis of Piled Raft Foundations). The reliability of the procedure to predict piled raft performance was then verified in nonlinear range by comparisons with both centrifuge tests and computer code PRAB.

Keywords: laterally loaded piles; piled raft; foundation; horizontal loading; nonlinearity; numerical analyses; pile; pile-soil interaction

1. Introduction

Behaviour of Combined Pile Raft Foundation (CPRF) under vertical loads has been largely investigated in recent years either via laboratory and field scale tests or via advanced numerical analysis.

It has been demonstrated that more rational design options are possible for vertically loaded piled raft (De Sanctis and Russo 2008, Ghiasi and Moradi 2018, Ko *et al.* 2018, Mandolini *et al.* 2005, 2013, Nakanishi and Takewaki 2013, Russo *et al.* 2013, Russo 2018, Sharafkhan *et al.* 2018) to enhance the collaboration among raft and piles, to increase the bearing capacity and to control absolute and differential settlement.

The Eurocode 7 (EC7-1 2004) and the ISSMGE Combined Pile Raft Foundation (CPRF) Guideline (Katzenbach and Choudhury 2013) permit since relatively long time to take profit of vertical load sharing between the piles and the raft which requires advanced methods of analysis. In the same documents no mention of CPRF subjected to transverse loads can be found. This fact reflects on the one hand the lack of knowledge about CPRF response under lateral loading and on the other the unavailability of computationally efficient codes for routine use in practice.

CPRF lateral response is characterized by the overlap of different mobilization mechanisms: the lateral resistance of the piles; the shear resistance at the raft-soil interface; the passive resistance of the soil in front of the raft, if the

connecting structure is embedded (Viggiani *et al.* 2012).

The key factors influencing the CPRF lateral response include the pile-head connection rigidity, the pile-soil relative stiffness, the pile spacing and the pile-soil, raft-soil, pile-pile, raft-pile interactions. Furthermore, full scale tests (Huang *et al.* 2001, O'Neill and Dunnavant 1984) failed to draw general conclusions about the influence of the execution technique.

Many experimental and numerical contributions (Hamada *et al.* 2015, Horikoshi *et al.* 2003, Matsumoto *et al.* 2010, 2004, Mokwa and Duncan 2001, Sawada and Takemura 2014, Unsever *et al.* 2014, 2015, Vu *et al.* 2016, 2017) show that the contribution offered by the raft-soil contact is significant and is also responsible for the decrease of bending moments on piles. However, further field or lab tests are still badly needed to increase the general understanding of the mechanism which govern the piled raft response under combined loading.

For the analysis of CPRFs the most widely used methods are BNWF (Beam on Nonlinear Winkler Foundation) approaches (i.e., p-y curves). Methods based on p-y curves (API 2007, Comodromos *et al.* 2016, Hirai 2012, Jamil and Ahmad 2019, Jeong and Cho 2014) are limited to the analysis of single pile problems where the subgrade soil reaction modulus is not an intrinsic soil parameter (Russo and Viggiani 2009). The use of p-y multipliers (Brown *et al.* 1988, McVay *et al.* 1998, Rollins *et al.* 2005) enables BNWF methods to be applied also in case of pile group and CPRF (Comodromos *et al.* 2016). p-y multipliers are used to scale the single pile transfer curves (p-y curves) and to introduce a stiffness reduction of these curves due to group effects. Several codes and analytical methods are based on p-y curves approach. Nevertheless,

*Corresponding author, Ph.D.

E-mail: stefano.stacul@for.unipi.it

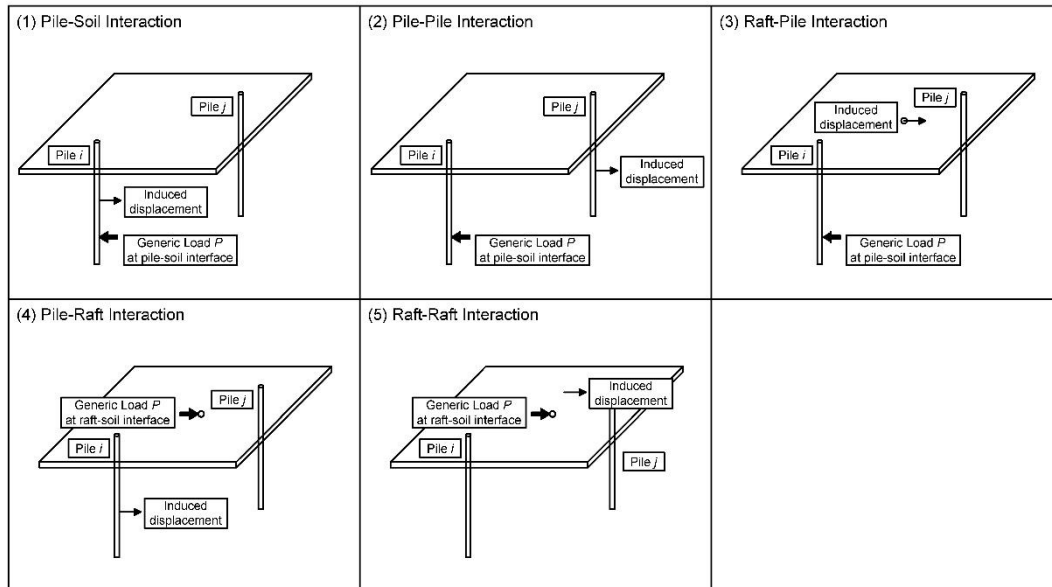


Fig. 1 Interactions modelled in PRaFULL

BNWF methods do not consider the soil as a continuum, this can be done by using BEM (Boundary Element Method) or FEM (Finite Element Method) (Plaxis BV 2015, Wu *et al.* 2015).

The diffusion of FEM for pile foundation applications is still limited by several modelling complexities (especially in the case of pile group and CPRF under lateral loading, which are non-axisymmetric problems), and as shown in Mardfekri *et al.* (2013) FEM calculations are influenced by even minor details of the modelling of the pile and its interface.

Therefore, FEM analyses have been used mainly for reference purposes to validate other simplified methods or to generate new load transfer curves (Yang and Jeremic 2002, 2003).

BEM approaches are less computationally demanding compared to FEM and allow pile-pile interactions to be directly assessed on the specific group composition and geometry considering, even if in a simplified way, the site-specific soil layering. Most of previously developed BEM codes are limited to pile group analysis if the lateral load case is considered (Basile 2015, Poulos 1999).

2. Proposed BEM code: PRaFULL

A method to study pile groups and CPRFs under lateral loading should be able to capture all the interactions between the piles, the raft and the soil accounting also for material nonlinearities (i.e., soil and concrete).

The originality of the proposed code, in the next called shortly PRaFULL (Piled Raft Foundation Under Lateral Load), lies in providing a complete Boundary Element Method solution for all the interactions via the soil modelled as a continuum considering several realistic features of the nonlinear behaviour of the materials involved.

The interactions modelled in PRaFULL are described in

Fig. 1 and are defined as follows:

- (1) Pile-Soil interaction: displacement induced at the pile-soil interface of a pile i by a load acting at the pile-soil interface of the same pile i ;
- (2) Pile-Pile interaction: displacement induced at the pile-soil interface of a pile j by a load acting at the pile-soil interface of another pile i ;
- (3) Raft-Pile interaction: displacement induced at the raft-soil interface by a load acting at the pile-soil interface of a generic pile i ;
- (4) Pile-Raft interaction: displacement induced at the pile-soil interface of a generic pile i by a load acting at the raft-soil interface;
- (5) Raft-Raft interaction: displacement induced at the raft-soil interface by a load acting at the raft-soil interface.

This code represents an extension to the piled raft case of a recently proposed analysis method for pile group (Stacul and Squeglia 2018). Compared to FEM a drastic reduction in computational resources for the analysis of full-scale 3D CPRFs under lateral load has to be recognized. The main assumptions in the code PRaFULL are here briefly listed:

- the interactions are accounted by using the Mindlin's and Cerutti's elastic solutions;
- multi-layered elastic soil is modelled by the approximation suggested in Poulos and Davis (1980);
- nonlinear behaviour is assumed for reinforced concrete (r.c.) sections (Morelli *et al.* 2017);
- nonlinear soil behaviour is accounted (incremental analysis) by a quasi-hyperbolic soil stiffness degradation curve (Fahey and Carter 1993, Stacul and Squeglia 2018);
- group effects (i.e., shadowing effect) are modelled using a Strain Wedge Model based approach (Ashour *et al.* 2004, Stacul and Squeglia 2018);
- the soil resistance distribution with depth (p_{ult}) is assessed according to the relationships suggested in

Matlock (1970), Reese *et al.* (1974, 1975), Welch and Reese (1972);

- the influence of vertical loads is considered using an improved version of the Poulos-Davis-Randolph (PDR) method (Poulos 2000, Poulos and Davis 1980, Randolph 1994);

- suction in shallower soil layers is accounted by using the modified Kovacs model (Aubertin *et al.* 2003, Stacul and Squeglia 2018).

2.1 Pile and soil modelling

The pile is modelled as a vertical strip $L \times D$, where D is the pile diameter and L is the length of the pile, discretized in slices with variable length with depth (Fig. 2).

The discretization was proposed after an optimisation exercise by Landi (2006) and was successfully used by Russo (2016), Stacul *et al.* (2017) and Stacul and Squeglia (2018).

The coefficients of the pile flexibility matrix are computed via the auxiliary constraint method (Fig. 3) as shown in the Eqs. (1a)-(1b).

$$a_{ij} = \frac{z_i^3}{3E_p I_p} + \frac{z_i^2(z_j - z_i)}{2E_p I_p} \quad \text{if } z_i < z_j \quad (1a)$$

$$a_{ij} = \frac{z_j^3}{3E_p I_p} + \frac{z_j^2(z_i - z_j)}{2E_p I_p} \quad \text{if } z_i \geq z_j \quad (1b)$$

where z_i is the abscissa of the centre of the generic slice i^{th} , E_p the Young's modulus of the pile and I_p the inertia of the pile transversal section.

Thus, the lateral displacement of each pile-slice is defined by the Eq. (2).

$$y_i = -\sum_{j=1}^n a_{ij} P_j + y_0 + \theta_0 z_i \quad (2)$$

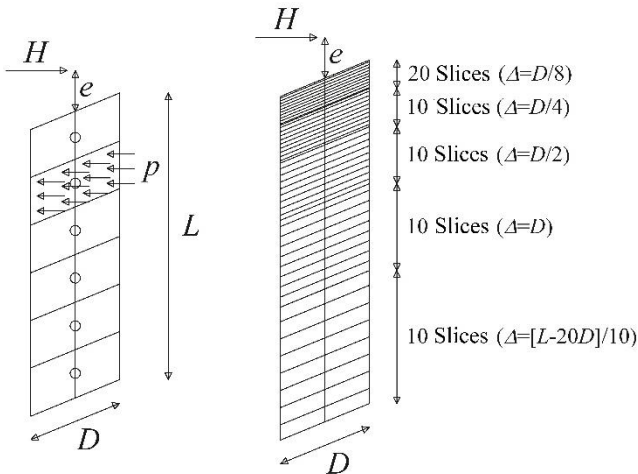


Fig. 2 Pile slices height with depth (Stacul and Squeglia 2018)

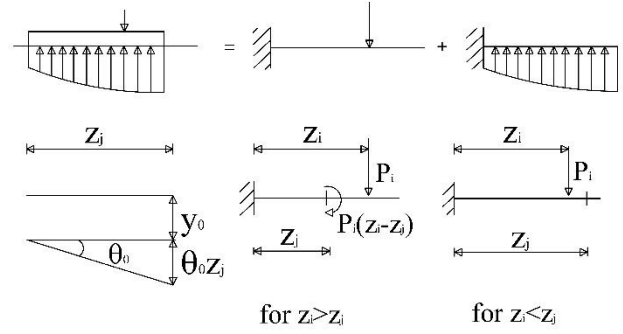


Fig. 3 Auxiliary constraint method (Stacul and Squeglia 2018)

where P_j is the resultant of the pile-soil interaction pressure on the generic pile-slice j , while y_0 and θ_0 are the rigid horizontal movement and rotation at the pile-head.

Obviously if the pile-head is perfectly fixed the rotation $\theta_0 = 0$ and it does not belong to the unknown list. The Eq. (2) establishes that the displacement of any slice j depends on $n+2$ or $n+1$ unknowns in case of free-head and fixed-head piles, respectively, n interface pressures p_j or their resultant, P_j , y_0 and θ_0 . The latter (θ_0) is zero for fixed-head piles.

PRaFULL can analyse both steel and r.c. piles. In the former case (steel pile), the flexural stiffness ($E_p I_p$) is considered constant unless the bending moment reaches the ultimate value for the selected section. In the latter case (r.c. sections) a nonlinear approach which considers even the influence of tension stiffening (Morelli *et al.* 2017) is used, to properly account the development of cracks.

The model allows to determine the moment-curvature relationship which is implemented in the code via a variable value of the inertia I_p (Stacul *et al.* 2017).

2.1.1 Pile-soil, pile-pile and raft-pile interactions

The soil is modelled as a multi-layered elastic halfspace and the Mindlin's solution (Mindlin 1936) is used to evaluate the pile-soil, pile-pile and raft-pile interactions. Nevertheless, the latter elastic solution is rigorously valid in the case of a homogeneous elastic halfspace. The multi-layered elastic halfspace is solved by means of the approximation suggested by Poulos and Davis (1980) and discussed by De Sanctis *et al.* (2002). The approximation consists in averaging the elastic moduli at the depths where the displacement is assessed and the load is applied, respectively, $E = (E_i + E_j)/2$. The lateral movement s_{ij} (at point i) induced by a lateral load P_j (at point j) is defined according to the Eq. (3) if $i \neq j$ (Fig. 4) while the displacement of an element due to its own loading (i.e., $i = j$) is computed by integrating the Mindlin's solution over a rectangular area as described in Douglas and Davis (1964).

$$s_{ij} = \frac{P_j(1+\nu)}{8\pi E_s(1-\nu)} \left[\frac{(3-4\nu)}{R_1} + \frac{1}{R_2} + \frac{x^2}{R_1^3} + \frac{3-4\nu}{R_2^3} x^2 + \frac{2cz}{R_2^3} \left(1 - \frac{3x^2}{R_2^2} \right) + \frac{4(1-\nu) \cdot (1-2\nu)}{R_2+z+c} \left(1 - \frac{x^2}{R_2(R_2+z+c)} \right) \right] = b_{ij} P_j \quad (3)$$

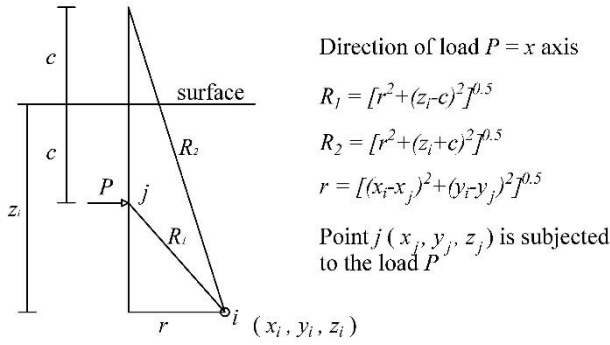


Fig. 4 Mindlin's solution scheme

It is useful to remark that nonlinear response of the system is simulated by means of an incremental analysis. Herein, the tangent elastic moduli of the layered soil (used in Eq. (3)) are updated at each step of the analysis based on the stress levels attained, according to the procedure described in section 2.1.3. Moreover, interface pressures are limited to fixed threshold values p_{ult} (e.g., Matlock 1970, Reese *et al.* 1974, 1975, Welch and Reese 1972). Once reached the latter values, interface pressures cannot further increase.

2.1.2 Pile-raft and raft-raft interactions

The raft is modelled as a thin plate discretized in n slices having a square shape and subjected to uniform shear stresses at each slice. Cerutti's solution is adopted to model pile-raft and raft-raft interactions. The approximation suggested by Poulos and Davis (1980) and described in the previous section for the multi-layered elastic halfspace is used. A generic load (P_j) applied at the point j along the raft-soil interface causes a horizontal movement ρ_{ij} at the point i belonging to the halfspace given by the Eq. (4) (Fig. 5).

$$\rho_{ij} = \frac{P_j(1+\nu)}{2\pi ER} \left[1 + \frac{x^2}{R^2} + (1-2\nu) \left(\frac{R}{R+z} - \frac{x^2}{(R+z)^2} \right) \right] = c_{ij} P_j \quad (4)$$

At the raft-soil interface the sliding mechanism will initiate when the shear stress at the interface exceeds a value defined by:

- a frictional law (Eq. (5a)) in drained conditions

$$\tau_f = \sigma_n \tan \delta \quad (5a)$$

where σ_n is obtained via the vertical load analysis that is described in the following pages (using an improved version of the Poulos-Davis-Randolph method (Poulos 2000, Poulos and Davis 1980, Randolph 1994)). δ is the angle of friction at the raft-soil interface that can be reasonably taken equal to 2/3 of the angle of internal friction of the superficial soil layer;

- an adhesion law (Eq. (5b)) in undrained conditions (total stress approach)

$$\tau_f = \beta \cdot s_u \quad (5b)$$

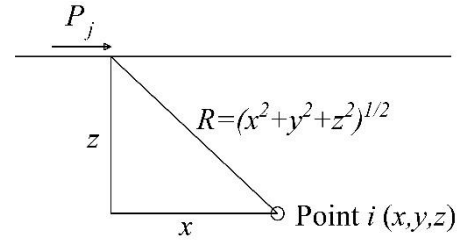


Fig. 5 Cerutti's solution scheme

where s_u is the soil undrained shear strength and β is a constant that should be properly selected.

Once reached the ultimate shear stress, at a raft-soil interface slice, relative sliding is allowed and for this slice the compatibility equation is neglected. Also in this case, the tangent elastic moduli in Eq. (4) are updated at each step of the analysis based on the stress levels attained.

2.1.3 Soil nonlinear behaviour

Several authors used hyperbolae to model shear stress-strain curves, with the tangent equal to G_{max} at zero strain and equal to 0 at τ_{max} corresponding to an infinite strain value. By defining a reference strain ($\gamma_{ref} = \tau_{max}/G_{max}$) it is possible to write the Eq. (6) describing the evolution of G_{sec} in the hypothesis that the shear-strain relationship is a hyperbola.

$$\frac{G_{sec}}{G_{max}} = \frac{1}{\left(1 + \frac{\gamma}{\gamma_{ref}} \right)} \quad (6)$$

In this work the nonlinear soil response is accounted by using a modified formulation of the original secant (Eq. (7)) and tangent (G_{tan}) (Eq. (8)) shear modulus degradation curves presented in Fahey and Carter (1993).

$$\frac{G_{sec}}{G_{max}} = 1 - \left(\frac{\tau}{\tau_{max}} \right)^g \quad (7)$$

$$\frac{G_{tan}}{G_{max}} = \frac{\left(\frac{G_{sec}}{G_{max}} \right)^2}{\left[1 - (1-g) \cdot \left(\frac{\tau}{\tau_{max}} \right)^g \right]} \quad (8)$$

In the Eqs. (7)-(8) the degradation curves are expressed as a function of shear stress rather than shear strain. These equations employ a coefficient g to define the shape of the curve. Typical values of g range between 0.25 and 1.0 and a procedure for its assessment is suggested in Stacul (2018) and Stacul and Squeglia (2018).

In PRaFULL the Eqs. (7)-(8) are modified replacing the "shear stress – maximum shear stress" ratio (τ/τ_{max}) with the "interface pressure – soil pressure at failure" ratio (p/p_{ult}) ratio, thus assuming constant the vertical stresses at the pile-soil interface during the lateral load analysis. This means that at each step of the lateral load analysis the G_{tan} value is updated at each interface slice using the Eqs. (7)-(8), in

which τ/τ_{max} is replaced by p/p_{ult} .

2.2 Vertical load applied over the raft

In PRaFULL code, the lateral contribution offered by the intrados of the raft in a piled raft system is activated when the raft is in contact with the ground. When a vertical load is applied in drained conditions a frictional strength is available while in undrained conditions a total stress approach is possible, and the contact is purely adhesive. Currently, the code is based on the following procedure:

- the vertical load is applied prior to the lateral one;
- the vertical load distribution among the piles and the raft is evaluated using the PDR method (Poulos 2000, Poulos and Davis 1980, Randolph 1994);
- the vertical load analysis is not coupled with the lateral load analysis. This means that the vertical load analysis is only performed to evaluate the vertical load sharing between raft and piles, and thus the induced vertical stress at each raft-soil interface slice;
- the vertical stress induced at each raft-soil interface element represents the σ_n value used in the Eq. (5a). This permits to compute the available shear resistance at each raft-soil interface slice; the vertical stress computed at each element of the raft-soil interface, is adopted for a further elastic calculation of the vertical additional stress to be added at the geostatic stress at any pile-soil interface element. This allows to increase the ultimate soil lateral resistance at each pile-soil interface element, computed using the expressions suggested in Matlock (1970), Reese *et al.* (1974, 1975) and Welch and Reese (1972);
- the vertical load distribution between the raft and the piles is kept constant during the monotonic increase of the lateral load analysis.

The vertical load analysis is performed using an improved version of the PDR method that can take also into account of the piled raft nonlinear response. The original method is described in an extended way in Poulos (2000).

The improved version of the PDR approach can be applied starting from the knowledge of the values of the raft stiffness (K_R), the raft bearing capacity ($Q_{R,lim}$), the pile group stiffness (K_G) and the single pile bearing capacity ($Q_{P,lim}$). Once these basic elements are known the full load-settlement curve of the piled raft foundation can be evaluated. The bearing capacity of the raft and of the single pile can be computed using the analytical formulae available in literature or experimental load test data.

The raft stiffness K_R is evaluated using the method proposed by Mayne and Poulos (1999) (Eq. (9)).

$$w_{raft} = \frac{qdI_G I_F (1-\nu^2)}{E_0} \quad (9)$$

where: q = applied stress; d = diameter of the raft foundation or an equivalent diameter if the raft is square/rectangular; E_0 = value of the soil modulus directly beneath the raft (at $z = 0$); ν = Poisson's ratio; I_G = influence factor for a Gibson soil profile (soil modulus linearly variable with depth) for both rigid and flexible

footings (Mayne and Poulos 1999); I_F = influence factor to consider the foundation flexibility (Mayne and Poulos 1999). I_F is expressed as a function of the foundation flexibility factor K_F , defined in Mayne and Poulos (1999) with the Eq. (10).

$$K_F \cong \frac{E_{fdn}}{E_{sAV}} \left(\frac{2t}{d} \right)^3 \quad (10)$$

where: d = foundation diameter; E_{fdn} = elastic modulus of the foundation material; E_{sAV} = representative elastic soil modulus located beneath the foundation base (i.e., value of E_s at depth $z = 0.5d$); t = foundation thickness.

The pile group stiffness K_G , instead, can be evaluated using the well-known interaction-coefficients approach proposed by Poulos and Davis (1980). A BEM solution obtained on a couple of identical piles is the base for the calculations of the interaction coefficient, α (Russo 1998). The settlement w_i of the generic pile i is calculated using the Eq. (11):

$$w_i = w_{1,i} (Q_i \alpha_{ii} + \sum Q_j \alpha_{ij}) \quad (11)$$

where: $w_{1,i}$ = settlement of the single pile subjected to a unit load; Q_j = vertical load acting on the generic pile j . The nonlinear response is considered with an incremental analysis, following the suggestions provided by Caputo and Viggiani (1984). In the simplified assumption that the raft is rigid in bending all the piles have the same settlement and n compatibility equations as the Eq. (11) can be written. $n+1$ unknowns are easily computed solving a system with $n+1$ equations, in which the additional is an equilibrium equation (Mandolini and Viggiani 1997).

The same concept is used also for the raft. This means that the raft stiffness is reduced at each load step of the incremental analysis by dividing the initial raft stiffness K_R with the coefficient α_{rr} (Eq. (12)).

$$\alpha_{rr} = \frac{1}{\left(1 - \frac{Q_R}{Q_{R,lim}} \right)^2} \quad (12)$$

In Eq. (12) Q_R is the vertical load acting on the raft at the previous load step and $Q_{R,lim}$ is the raft bearing capacity. Once all the ingredients are determined an incremental solution of the load sharing can be obtained taking the last step as the only significant result to be used for the analysis of the piled raft under lateral loading.

2.3 General system of equations

At each step of the incremental lateral load analysis, the code PRaFULL solves the system of equations $[A][X] = [B]$ presented in detail in the Eq. (13).

The system of equations is composed of compatibility equations (on the displacement at the pile-soil and the raft-soil interface) and equilibrium equations to lateral translation and to rotation. Two extreme cases can be analysed: free-head and fixed-head piles. The nonlinear analysis is performed by adopting an incremental approach,

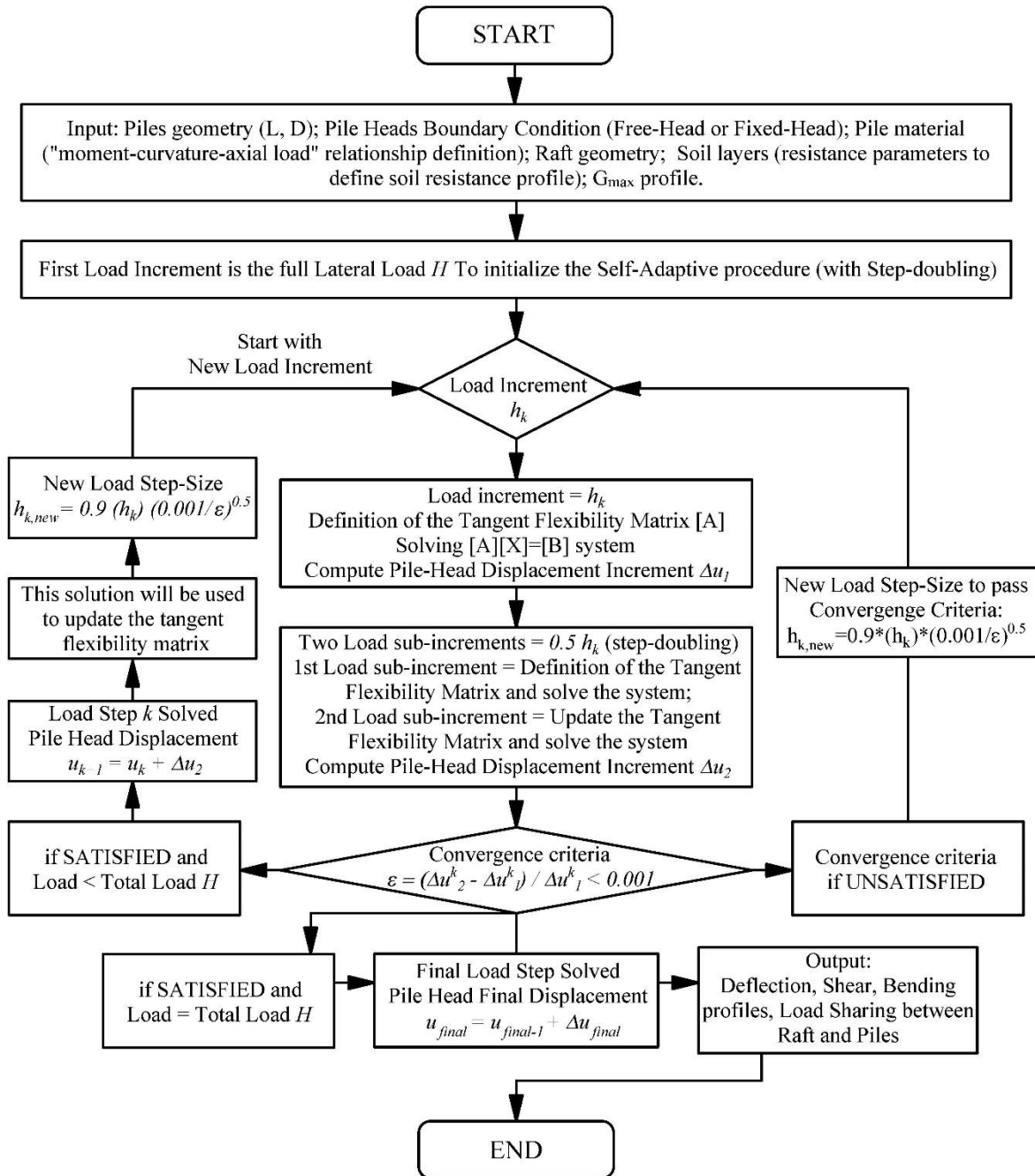


Fig. 6 Iterative scheme to solve each step of the analysis with PRAFULL

using an adaptive step-size control.

For a foundation with m piles subdivided in n slices and a connecting raft subdivided in r elements, the column vector $[X]$ is composed of $nm+r+2m+2$ or $nm+r+m+2$ unknowns terms in case of free-head or fixed head piles, respectively, p are the $nm+r$ unknown pile-soil interface pressures (p^p) and raft-soil interface pressures (p^r), y_0 is the CPRF lateral movement, θ_m and H_m are the m rotations and m horizontal loads at each pile-head, respectively, and H_{raft} is the horizontal load carried by the raft. $[B]$ is a column vector including the known terms of the problem, while $[A]$ is a $(nm+r+2m+2) \times (nm+r+2m+2)$ or $(nm+r+m+2) \times (nm+r+m+2)$ matrix, in case of free-head and fixed-head

piles, respectively, obtained by adding:

- the $nm \times nm$ matrix $[A_P]$, where $[A_P]$ consists of the a_{ij} coefficients (Eq. (1)) representing the pile flexibility;
- the $nm \times nm$ matrix $[A_S]$, where $[A_S]$ consists of the b_{ij} coefficients (Eq. (3)) representing the interactions (1) and (2) in Fig. (1);
- the $r \times nm$ matrix $[A_{SR}]$, where $[A_{SR}]$ consists of the d_{ij} coefficients representing the interaction (3) in Fig. (1) and computed with the Eq. (3) in which b_{ij} is replaced by d_{ij} ;
- the $nm \times r$ matrix $[A_{RS}]$, where $[A_{RS}]$ consists of the

c_{ij} coefficients (Eq. (4)) representing the interaction (4) in Fig. (1);

- the $r \times r$ matrix $[A_{RR}]$, where $[A_{RR}]$ consists of the e_{ij} coefficients (Eq. (4)) representing the interaction (5) in Fig. (1).

The final $2m+2$ or $m+2$ rows and columns of the $[A]$ matrix (Eq. (13)) define the equilibrium equations and complete the displacement compatibility equations, respectively. In the Eq. (13) Δ_i is the height (Fig. 2) of the generic slice i^{th} of the pile and Δ_r is the width of each squared element in which the raft-soil interface has been discretized, while H and f are the applied lateral load and the load eccentricity, respectively. The load eccentricity is referred to the ground surface and applicable only for the free head case. The matrix $[A]$ is updated at each step of the lateral load analysis if pile or soil nonlinear response is considered. The pile flexibility sub-matrix $[A_P]$ is updated based on the moment-curvature curve of the pile section and the bending moments reached at each pile-node in the previous load increment by updating the values of a_{ij} coefficients in Eq. (13). The moment-curvature relationship of a typical reinforced concrete circular section is inferred via the procedure described in Morelli *et al.* (2017). Once the latter has been defined the pile is modelled as a step-tapered beam with a variable flexural rigidity ($E_p I_p$) along its own axis as a function of the attained curvature. As a consequence, a_{ij} coefficients have to be computed as shown in Stacul and Squeglia (2018). Moreover, at each load step a check is carried out to determine if the soil pressure at failure has been reached at each pile-soil and raft-soil interface. When it happens at that node the compatibility equation is removed. The procedure described in Fig. 6 shows that at each lateral load increment h_k , an iterative process is followed where two solutions are obtained, the first using h_k , the second using two load sub-increments equal to $h_k/2$. This scheme refers to the explicit Euler method with step-doubling and adaptive step-size control (Press *et al.* 1992). As an alternative a fourth order Runge-Kutta method can be used to increase the solution accuracy.

3. Validation of PRaFULL code

3.1 Validation against other codes: linearly elastic solutions

In this section the results of two linear elastic parametric studies on piled raft foundations subjected to lateral load are shown. Comparison is made with solutions by a well-known existing code, called APRAF (Small and Zhang 2000, 2002, Small *et al.* 2006, Zhang and Small 2000) and based on the finite layer theory (Small and Booker 1986).

The first parametric study was carried out on a square piled raft foundation with 16 (4×4) piles embedded in a deep uniform soil with a Poisson's ratio of the soil $\nu_s = 0.35$ and the soil modulus, $E_s = 10$ MPa. The piles were 15 m long and the pile diameter D was 0.5 m, and the pile-heads fixed against the rotation.

To evaluate the effect of the pile-soil stiffness ratio (E_p/E_s) on the load distribution (between the 4×4 pile-group and the raft) and on the displacement the analyses were carried out using a pile spacing ratio, s/D , equal to 5, while the pile-soil stiffness ratio, E_p/E_s , was taken equal to: 10, 100, 1000, 10000. The normalized horizontal displacement in the work of Small and Zhang (2000) was defined using the Eq. (14).

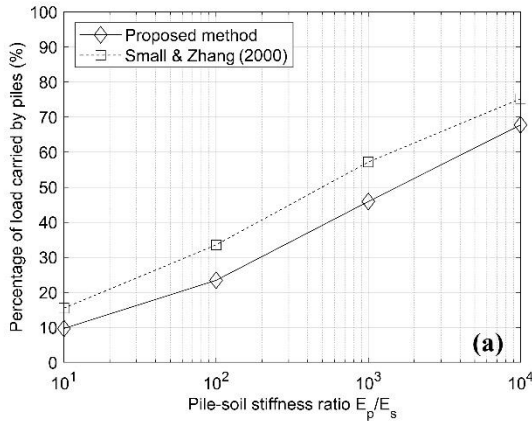
$$I_{u,xx} = \frac{E_s D y}{H} \quad (14)$$

where y is the piled raft lateral displacement and H the lateral load.

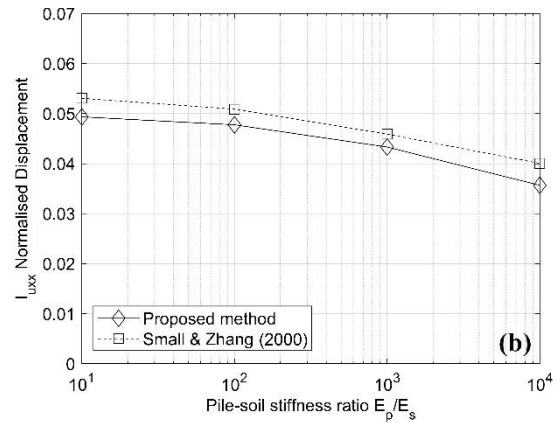
The results (Figs. 7(a) and 7(b)) are compared with those obtained by Small and Zhang (2000) using the code APRAF. The normalized movement $I_{u,xx}$ of the piled raft reduces as the ratio E_p/E_s increases, while the load carried by the 4×4 pile group increases as the ratio E_p/E_s increases, with both codes (PRaFULL and APRAF).

Moreover, the effect of s/D on the load distribution (between the 4×4 pile-group and the raft) and on the displacement, was examined. The analyses were carried out

$$\begin{bmatrix} a_{1,1} + b_{1,1} & \cdots & a_{1,mm} + b_{1,mm} & c_{1,1} & \cdots & c_{1,r} & -1 & -z_{1,1} & \cdots & \cdots & 0 & \cdots & 0 & 0 \\ \vdots & \ddots & \vdots & \vdots & \ddots & \vdots & \vdots & \vdots & \ddots & \vdots & \vdots & \ddots & \vdots & \vdots \\ a_{nm,1} + b_{nm,1} & \cdots & a_{nm,mm} + b_{nm,mm} & c_{nm,1} & \cdots & c_{nm,r} & -1 & \cdots & \cdots & -z_{nm,m} & 0 & \cdots & 0 & 0 \\ d_{1,1} & \cdots & d_{1,mm} & e_{1,1} & \cdots & e_{1,r} & -1 & 0 & \cdots & 0 & 0 & \cdots & 0 & 0 \\ \vdots & \ddots & \vdots & \vdots & \ddots & \vdots & \vdots & \vdots & \ddots & \vdots & \vdots & \ddots & \vdots & \vdots \\ d_{r,1} & \cdots & d_{r,mm} & e_{r,1} & \cdots & e_{r,r} & -1 & 0 & \cdots & 0 & 0 & \cdots & 0 & 0 \\ 1 & \cdots & 1 & 1 & \cdots & 1 & 0 & 0 & \cdots & 0 & 0 & \cdots & 0 & 0 \\ z_{1,1} & \cdots & \cdots & 0 & \cdots & 0 & 0 & 0 & \cdots & 0 & 0 & f & f & f \\ \vdots & \ddots & \vdots & \vdots & \ddots & \vdots & \vdots & \vdots & \ddots & \vdots & \vdots & f & 0 & f & f \\ \cdots & \cdots & z_{m,mm} & 0 & \cdots & 0 & 0 & 0 & \cdots & 0 & f & f & 0 & f & \theta_m \\ 1_{1,1} & \cdots & \cdots & 0 & \cdots & 0 & 0 & 0 & \cdots & 0 & -1 & 0 & 0 & 0 & H_1 \\ \vdots & \ddots & \vdots & \vdots & \ddots & \vdots & \vdots & \vdots & \ddots & \vdots & 0 & -1 & 0 & 0 & \vdots \\ \cdots & \cdots & 1_{m,mm} & 0 & \cdots & 0 & 0 & 0 & \cdots & 0 & 0 & 0 & -1 & 0 & H_m \\ 0 & \cdots & 0 & 1 & \cdots & 1 & 0 & 0 & \cdots & 0 & 0 & \cdots & 0 & -1 & H_{raft} \end{bmatrix} \begin{bmatrix} p_1^p \Delta_1 D \\ \vdots \\ p_{nm}^p \Delta_{nm} D \\ p_1^r \Delta_r^2 \\ \vdots \\ p_r^r \Delta_r^2 \\ y_0 \\ \theta_1 \\ \vdots \\ \theta_m \\ H_1 \\ \vdots \\ H_m \\ H_{raft} \end{bmatrix} = \begin{bmatrix} 0 \\ \vdots \\ 0 \\ 0 \\ \vdots \\ 0 \\ H \\ fH \\ \vdots \\ fH \\ 0 \\ \vdots \\ 0 \\ 0 \end{bmatrix} \quad (13)$$

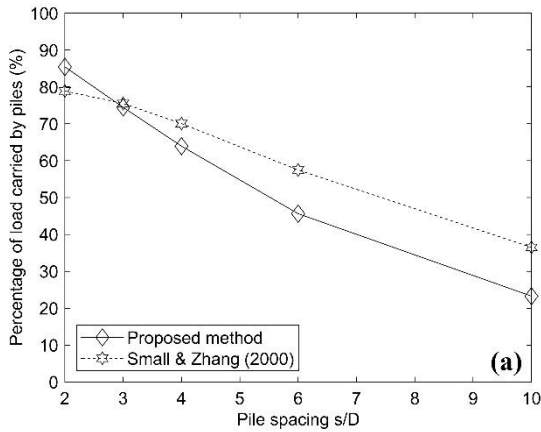


(a) Influence of E_p/E_s on the loading rate carried by the 4×4 pile group

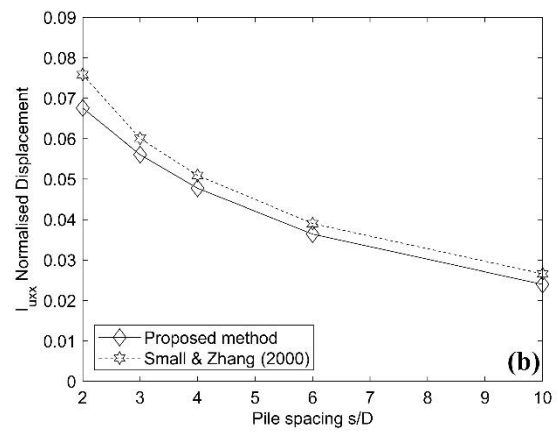


(b) Influence of E_p/E_s on the normalized displacement $I_{u,xx}$

Fig. 7 Influence of pile-soil stiffness ratio E_p/E_s

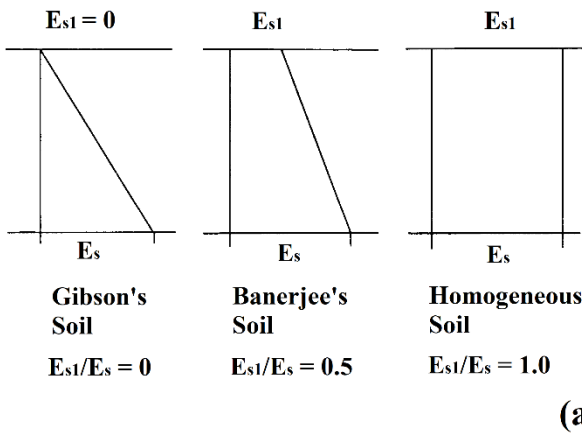


(a) Influence of s/D on: the loading rate carried by the piles

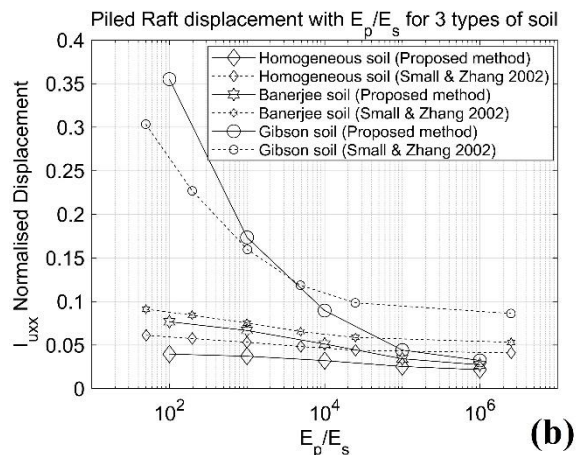


(b) Influence of s/D on the normalized displacement $I_{u,xx}$

Fig. 8 Influence of relative spacing s/D



(a) Soil types used in the parametric study no. 2



(b) Influence of E_p/E_s on $I_{u,xx}$ for three types of soil

Fig. 9 Influence of soil modulus distribution with depth

using a pile-soil stiffness ratio equal to 2000, while the pile spacing values investigated were: $2D$, $3D$, $4D$, $6D$ and $10D$. The results (Figs. 8(a) and 8(b)) are compared with those obtained by Small and Zhang (2000) using the code

APRAF. The increase of s/D has a significant influence on $I_{u,xx}$ and causes an important reduction of the horizontal loading rate carried by the 4×4 pile group.

The differences between APRAF and PRaFULL can be

justified even by different approximations and implementations while in general terms there is also a rather remarkable different model for the solution of the layered soil profiles.

Furthermore, looking at the results of Fig. 8a, it is possible to judge as not reliable the trend obtained by APRAF for pile spacing values less than 4. In fact, the loading rate carried by the pile group seems to reach an asymptotic value (approximately equal to 80%) for small pile spacings, while 100% is the only reasonable expectation for the limiting case of a pile spacing equal to 1.

The second parametric study was carried out on a square piled raft foundation with 16 (4×4) piles embedded in three different soil profiles. The Poisson's ratio ν_s and the elastic Young's modulus E_s (at the pile tip) of the soil together with the piles' slenderness ratio L/D were kept constant and respectively equal to 0.35, 30 MPa and 18.75. The pile diameter was 1.0 m and in this case the pile-heads were fixed against the rotation. To evaluate the effect of a variable pile-soil stiffness ratio E_p/E_s (100, 1000, 10000, 100000) on the displacement, the analyses were carried out using a constant spacing, $s/D = 6$. The three different soil profiles are sketched in Fig. 9(a) ($E_{s1}/E_s = 0$, $E_{s1}/E_s = 0.5$ and $E_{s1}/E_s = 1.0$; E_{s1} is the soil modulus at $z = 0$).

In the evaluation of the normalized horizontal displacement ($I_{u,xx}$) the E_s value at the pile tip is considered. The influence of E_p/E_s on the normalized displacement $I_{u,xx}$ is shown Fig. 9(b). It may be seen that the maximum displacement occurs in the Gibson's soil, while the minimum occurs in the case of the homogeneous soil. The increase of E_p/E_s in the Gibson's soil causes a relevant reduction of $I_{u,xx}$. The differences between APRAF and PRaFULL results in terms of normalised displacements (Fig. 7(b), 8(b) and 9(b)) are in most of the cases limited to the 10% which is a rather low value, while are higher in terms of load sharing (Fig. 7(a) and 8(a)). On the overall, the good agreement between the results obtained by the two codes shows that PRaFULL, even based on a very simple and easy to handle approximation, solves piled rafts embedded in heterogeneous soil profiles.

3.2 Validation on a case study

Horikoshi *et al.* (2003) published a series of static loading tests which were conducted vertically and laterally on piled raft models and on their basic components (single piles and rafts alone) embedded in sandy layer by using a geotechnical centrifuge. The influence of the pile head constraint on the overall piled raft behaviour was also investigated.

All the models (single pile, raft alone and piled rafts) were loaded in separate tests. The adopted centrifuge had an effective radius of 2.65 m while a centrifugal acceleration of 50g was applied to a 1/50 sized model. A rigid box 700 mm long, with a width of 400 mm and a height of 700 mm was used and Teflon sheets were purposely attached to the side-walls to reduce the wall friction. The analyses with PRaFULL code were conducted as a class A prediction in order to validate the proposed code, directly using the actual pile mechanical and geometrical properties, and the proposed procedure to derive the soil strength and stiffness

Table 1 Properties of the soil (Horikoshi *et al.* 2003)

Density of soil particle, ρ_s (ton/m ³)	2.661
Maximum dry density, $\rho_{d,max}$ (ton/m ³)	1.654
Minimum dry density, $\rho_{d,min}$ (ton/m ³)	1.349
Median grain size, D_{50} (mm)	0.162

Table 2 Properties of model pile and corresponding prototype pile (Horikoshi *et al.* 2003)

Item	Centrifuge model	Prototype
Material	Aluminium	Concrete
Outer diameter, D (mm)	10.0	500.0
Wall thickness, t (mm)	1.0	Solid
Length, L (mm)	180.0	9000.0
Cross sectional stiffness, $E_p A$ (GN)	0.002	5.0
Flexural stiffness, $E_p I_p$ (GNm ²)	2.0×10^{-8}	0.13
Young's modulus, E_p (GN/m ²)	71.0	41.7

parameters by the available laboratory tests data presented in the next section. The soil modulus (E) is intended as a soil modulus at small strain level (E_{max}). The latter can be defined starting from shear modulus at small strain level simply using the relationship: $E = 2G(1 + \nu)$. The available load-displacement relationship for the single pile case (Horikoshi *et al.* 2003) was used within a trial and error procedure with the best fit aim to estimate the exponent g of the modulus reduction curve (Eqs. (7)-(8)).

3.2.1 Soil conditions, raft and pile properties

The centrifuge tests were carried out filling the box with air-pluviated dry Toyoura sand (Table 1). The relative density (D_r) of the sand was about 60% after applying the centrifugal acceleration of 50g (before starting the horizontal test).

Triaxial tests were performed on soil specimens having relative density $D_r = 65\%$. The triaxial CD tests were conducted using 4 different confining pressures (50, 100, 200, 300 kPa). The peak friction angle was determined on the average as $\phi' = 45^\circ$. The measured values of G_{max} were closely fitted by the Eq. (15).

$$G_{max} = G_{ref} \left(\frac{p}{p_{ref}} \right)^{0.5} \quad (15)$$

where p_{ref} is a reference value of the confining pressure (and equal to 100 kPa) and G_{ref} is the value of G_{max} at $p = p_{ref}$. The value of G_{ref} was 21.08 MPa for a relative density equal to 65%, as shown in Matsumoto *et al.* (2004).

A square aluminium raft with width of 80 mm (4 meters at prototype scale) was used. The vertical load was simply applied by using a specified raft mass in the horizontal loading tests. The model pile was an aluminium pipe with an outer diameter of 10 mm, a wall thickness of 1 mm and an embedded length of 180 mm. The properties of the model and prototype pile are summarized in Table 2. The model pile closely represents a concrete pile with a

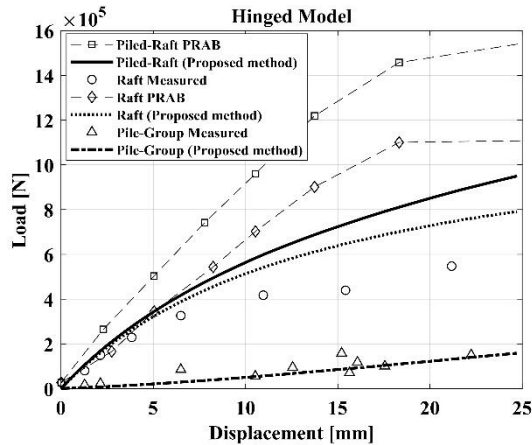


Fig. 10 Computed vs. measured load – displacement curve for the hinge piled raft model (results in prototype scale)

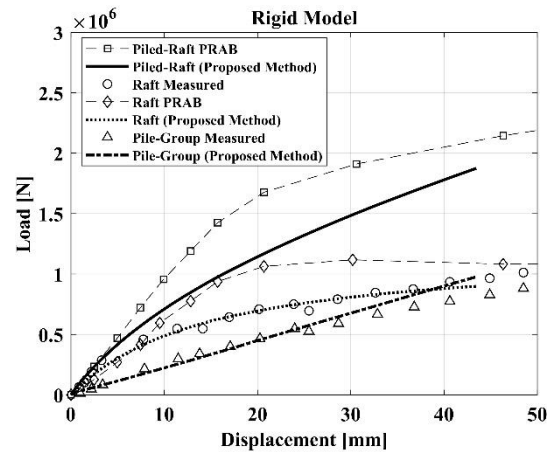


Fig. 12 Computed vs. measured load – displacement curve for the rigid piled raft model (results in prototype scale)

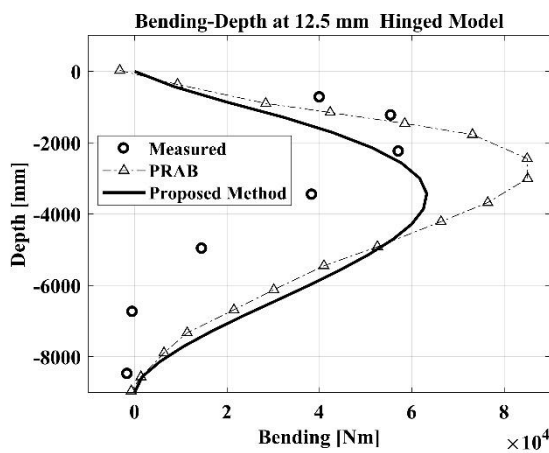


Fig. 11 Computed vs. measured distributions of bending moments along the pile shaft of a rear pile in the hinged piled raft model (results in prototype scale)

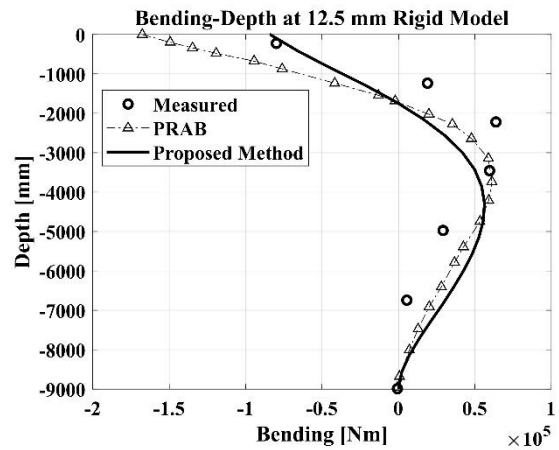


Fig. 13 Computed vs. measured distributions of bending moments along the pile shaft of a rear pile in the rigid piled raft model (results in prototype scale)

diameter of 500 mm at prototype scale. In Horikoshi *et al.* (2003), the pile head connections were set at the two extreme conditions: fixed and hinged. The raft base was roughened to increase the frictional resistance. Four piles were installed beneath the raft at a relative spacing of 4 diameters. The piled raft was horizontally loaded at a height of 25 mm above the soil surface and added mass was set above the raft to provide the desired vertical load to the piled raft model. The total weight of the raft was 2298 N at 50g and the ‘horizontal load-displacement’ relationship obtained in the raft alone lateral loading test permitted to estimate a coefficient of friction of 0.423 (i.e., a raft-soil interface friction angle of 22.9 degrees).

3.2.2 Analysis results: Hinged Piled Raft model

Based on the above outlined procedure the stiffness and shear strength parameters of the soil were determined. The soil pressure at failure distribution with depth was computed according to Reese *et al.* (1975). The vertical load distribution between the raft and the pile group before the lateral load test was an information provided in

Horikoshi *et al.* (2003). Measured and computed results are compared in terms of load vs. displacement curves of the hinged piled raft and its components (raft and pile group) (Fig. 10) and in terms of the rear pile bending moment profile at a displacement equal to 12.5 mm (Fig. 11).

In these figures the comparison is shown even against the results obtained by Kitiyodom *et al.* (2005) using the widely known code PRAB (Kitiyodom and Matsumoto 2002). It is worthwhile to remember that PRAB is a plate-beam-spring model in which the raft is modelled as thin plates, the pile via the elastic beam theory, the soil with horizontal and vertical springs. PRAB models the interactions between the structural elements with the Mindlin’s solutions and approximates the nonlinear soil behavior by employing an elastic-perfectly plastic response of the springs. The results shown reveal the ability of PRaFULL code to reproduce qualitatively and quantitatively the hinged piled raft response under horizontal loading. Particularly evident is the good agreement between the Raft curves and the Pile-Group curves respectively obtained by the proposed code and the experimental results. The PRAB results are by far less

compatible with the observed results.

3.2.3 Analysis results: Rigid Piled Raft

Measured and computed results are compared in terms of load vs. displacement curves of the fixed piled raft and its components (raft and pile group) (Fig. 12) and in terms of the rear pile bending moment profiles at a displacement equal to 12.5 mm (Fig. 13).

In these figures the comparison is shown even against the results obtained by Kitiyodom *et al.* (2005) using the code PRAB. The results highlight the possibility of providing a good prediction of: piled raft displacement, 'raft-pile group' load sharing and pile bending moment distribution with depth.

It is worth mentioning that the analyses with PRaFULL were carried out as class A prediction, using the actual pile and soil properties inferred by the laboratory tests.

The analysis results provided by Kitiyodom *et al.* (2005) were obtained using the plate-beam-spring model (code PRAB) where the soil is treated as springs and the nonlinear behaviour is modelled using an elastic-perfectly plastic response of the springs.

Moreover, the PRAB results are the outcomes of a back-analysis process where the soil modulus was varied to attain the best fitting with the measured load-displacement curves.

4. Conclusions

A laterally loaded CPRF represents a soil-structure interaction issue characterized by many sources of nonlinearities affecting both the soil and the structural elements. The possibility to reproduce the change in pile-soil relative stiffness while applying a lateral load is relevant for a proper assessment of the CPRF lateral response. Currently, most of the computer codes are specialized to solve separately geotechnical or structural problems.

For these reasons, a new BEM base code, called PRaFULL, has been presented here to study piled raft under horizontal loading taking into account most important features of the behaviour of both soil and pile material. Currently, it is possible to analyse two extreme cases: piles free-to-rotate or piles with fixed-head. An intermediate constraint can be also added.

The proposed method is innovative compared to existing codes because it considers among the sources of nonlinearity even the tension stiffening for the concrete section.

Furthermore, the shadowing effect on the ultimate soil pressure is also accounted, when dealing with pile groups and piled rafts, and a coupling effect between vertical and horizontal loading is considered: i.e., the influence of vertical load on the available shear strength at the raft soil interface.

PRaFULL has two following advantages compared to FDM and FEM codes:

- minor computational resources (less than 10 minutes for the entire load – displacement curve of a laterally loaded CPRF with a 4×4 pile group, by using an Intel i7 laptop);
- the definition of a relatively low number of pile and

soil properties as input.

PRaFULL solutions accuracy were first checked by comparing results from parametric studies carried out with a more complex and rigorous code (APRAF, Zhang and Small 2000) used as a benchmark. The check was satisfactorily. A comparison with experimental data on a piled raft laterally loaded in a centrifuge test program realized by Horikoshi *et al.* (2003) is finally presented. This comparison confirms the capabilities of PRaFULL in forecasting the key aspects of the piled raft response, i.e., load-displacement curve and pile bending moment distribution with depth. In this case the comparison was also done with the results of another computer code (PRAB) showing a better performance of the code proposed in this paper.

References

- API (2007), *Recommended Practice for Planning, Designing and Constructing Fixed Offshore Platforms — Working Stress Design. vol. 24–WSD*, American Petroleum Institute, U.S.A.
- Ashour, M., Pilling, P. and Norris, G. (2004), "Lateral behavior of pile groups in layered soils", *J. Geotech. Geoenviron. Eng.*, **130**(6), 580-592. [https://doi.org/10.1061/\(ASCE\)1090-0241\(2004\)130:6\(580\)](https://doi.org/10.1061/(ASCE)1090-0241(2004)130:6(580)).
- Aubertin, M., Mbonimpa, M., Bussière, B. and Chapuis, R.P. (2003), "A model to predict the water retention curve from basic geotechnical properties", *Can. Geotech. J.*, **40**(6), 1104-1122. <https://doi.org/10.1139/t03-054>.
- Basile, F. (2015), "Non-linear analysis of vertically loaded piled rafts", *Comput. Geotech.*, **63**, 73-82. <https://doi.org/10.1016/J.COMPGeo.2014.08.011>.
- Brown, D.A., Morrison, C. and Reese, L.C. (1988), "Lateral load behavior of pile group in sand", *J. Geotech. Eng.*, **114**, 1261-1276. [https://doi.org/10.1061/\(ASCE\)0733-9410\(1988\)114:11\(1261\)](https://doi.org/10.1061/(ASCE)0733-9410(1988)114:11(1261)).
- Caputo, V. and Viggiani, C. (1984), "Pile foundation analysis: A simple approach to nonlinearity effects", *Rivista Italiana Di Geotecnica*, **18**(1), 32-51.
- Comodromos, E.M., Papadopoulou, M.C. and Laloui, L. (2016), "Contribution to the design methodologies of piled raft foundations under combined loadings", *Can. Geotech. J.*, **53**(4), 559-577. <https://doi.org/10.1139/cgj-2015-0251>.
- De Sanctis, L. and Russo, G. (2008), "Analysis and performance of piled rafts designed using innovative criteria", *J. Geotech. Geoenviron. Eng.*, **134**, 1118-1128. [https://doi.org/10.1061/\(ASCE\)1090-0241\(2008\)134:8\(1118\)](https://doi.org/10.1061/(ASCE)1090-0241(2008)134:8(1118)).
- De Sanctis, L., Russo, G. and Viggiani, C. (2002), "Piled rafts on layered soils", *Proceedings of the DFI Symposium on Pile Foundations*, Nice, France.
- Douglas, D.J. and Davis, E.H. (1964), "The movement of buried footings due to moment and horizontal load and the movement of anchor plates", *Geotechnique*, **14**(2), 115-132.
- Eurocode (2004), *EC7-1, Eurocode 7 - Geotechnical design - Part 1: General rules*, European Committee for Standardization, Brussels, Belgium.
- Fahey, M. and Carter, J. (1993), "A finite element study of the pressuremeter test in sand using a nonlinear elastic plastic model", *Can. Geotech. J.*, **30**, 348-362. <https://doi.org/10.1139/t93-029>.
- Ghiasi, V. and Moradi, M. (2018), "Assessment the effect of pile intervals on settlement and bending moment raft analysis of piled raft foundations", *Geomech. Eng.*, **16**(2), 187-194. <https://doi.org/10.12989/gae.2018.16.2.187>.

- Hamada, J., Tsuchiya, T., Tanikawa, T. and Yamashita, K. (2015), "Lateral loading tests on piled rafts and simplified method to evaluate sectional forces of piles", *Geotech. Eng. J. SEAGS AGSSEA*, **46**, 29-42.
- Hirai, H.A. (2012), "Winkler model approach for vertically and laterally loaded piles in nonhomogeneous soil", *Int. J. Numer. Anal. Meth. Geomech.*, **36**, 1869-1897. <https://doi.org/10.1002/nag.1078>.
- Horikoshi, K., Matsumoto, T., Hashizume, Y., Watanabe, T. and Fukuyama, H. (2003), "Performance of piled raft foundations subjected to static horizontal loads", *Int. J. Phys. Modell. Geotech.*, **3**(2), 37-50. <https://doi.org/10.1680/ijpmg.2003.030204>.
- Huang, A.B., Hsueh, C.K., O'Neill, M.W., Chern, S. and Chen, C. (2001), "Effects of construction on laterally loaded pile groups", *J. Geotech. Geoenviron. Eng.*, **127**(5), 385-397. [https://doi.org/10.1061/\(ASCE\)1090-0241\(2001\)127:5\(385\)](https://doi.org/10.1061/(ASCE)1090-0241(2001)127:5(385)).
- Jamil, I. and Ahmad, I. (2019), "Bending moments in raft of a piled raft system using Winkler analysis", *Geomech. Eng.*, **18**(1), 41-48. <https://doi.org/10.12989/gae.2019.18.1.041>.
- Jeong, S. and Cho, J. (2014), "Proposed nonlinear 3-D analytical method for piled raft foundations", *Comput. Geotech.*, **59**, 112-126. <https://doi.org/10.1016/j.compgeo.2014.02.009>.
- Katzenbach, R. and Choudhury, D. (2013), "ISSMGE Combined Pile-Raft Foundation (CPRF) Guideline", Technische Universität Darmstadt, Germany.
- Kitiyodom, P. and Matsumoto, T. (2002), "A simplified analysis method for piled raft and pile group foundations with batter piles", *Int. J. Numer. Anal. Meth. Geomech.*, **26**(13), 1349-1369. <https://doi.org/10.1002/nag.248>.
- Kitiyodom, P., Matsumoto, T., Horikoshi, K. and Watanabe, T. (2005), "Analyses of vertical and horizontal load tests on piled raft models in dry sand", *Proceedings of the International Conference on Soil Mechanics and Geotechnical Engineering*, Osaka, Japan, September.
- Ko, J., Cho, J. and Jeong, S.S. (2018), "Analysis of load sharing characteristics for a piled raft foundation", *Geomech. Eng.*, **16**(4), 449-461. <https://doi.org/10.12989/gae.2018.16.4.449>.
- Landi, G. (2006), "Pali soggetti a carichi orizzontali: indagini sperimentali ed analisi", Ph.D. Dissertation, University of Naples Federico II, Naples, Italy (in Italian).
- Mandolini, A. and Viggiani, C. (1997), "Settlement of piled foundations", *Géotechnique*, **47**(4), 791-816. <https://doi.org/10.1680/geot.1997.47.4.791>.
- Mandolini, A., Di Laora, R. and Mascarucci, Y. (2013), "Rational design of piled raft", *Proc. Eng.*, **57**, 45-52. <https://doi.org/10.1016/j.proeng.2013.04.008>.
- Mandolini, A., Russo, G. and Viggiani, C. (2005), "Pile foundations: Experimental investigations, analysis and design", *Proceedings of the International Conference on Soil Mechanics and Geotechnical Engineering*, Osaka, Japan, September.
- Mardfekri, M., Gardoni, P. and Roesset, J.M. (2013), "Modeling laterally loaded single piles accounting for nonlinear soil-pile interactions", *J. Eng.*, 1-7. <https://doi.org/10.1155/2013/243179>.
- Matlock, H. (1970), *Correlations for Design of Laterally Loaded Piles in Soft Clay*, in *Offshore Technology in Civil Engineering: Hall of Fame Papers from the Early Years*, ASCE, 77-94.
- Matsumoto, T., Fukumura, K., Pastsakorn, K., Horikoshi, K. and Oki, A. (2004), "Experimental and analytical study on behaviour of model piled rafts in sand subjected to horizontal and moment loading", *Int. J. Phys. Modell. Geotech.*, **4**(3), 1-19. <https://doi.org/10.1680/ijpmg.2004.040301>.
- Matsumoto, T., Nemoto, H., Mikami, H., Yaegashi, K., Arai, T. and Kitiyodom, P. (2010), "Load tests of piled raft models with different pile head connection conditions and their analyses", *Soils Found.*, **50**(1), 63-81. <https://doi.org/10.3208/sandf.50.63>.
- Mayne, P.W. and Poulos, H.G. (1999), "Approximate displacement influence factors for elastic shallow foundations", *J. Geotech. Geoenviron. Eng.*, **125**(6), 453-460. [https://doi.org/10.1061/\(ASCE\)1090-0241\(1999\)125:6\(453\)](https://doi.org/10.1061/(ASCE)1090-0241(1999)125:6(453)).
- McVay, M., Zhang, L., Molnit, T. and Lai, P. (1998), "Centrifuge testing of large laterally loaded pile groups in sands", *J. Geotech. Geoenviron. Eng.*, **124**(10), 1016-1026. [https://doi.org/10.1061/\(ASCE\)1090-0241\(1998\)124:10\(1016\)](https://doi.org/10.1061/(ASCE)1090-0241(1998)124:10(1016)).
- Mindlin, R.D. (1936), "Force at a point in the interior of a semi-infinite solid", *Physics*, **7**, 195-202. <https://doi.org/10.1063/1.1745385>.
- Mokwa, R.L. and Duncan, J.M. (2001), "Experimental evaluation of lateral-load resistance of pile caps", *J. Geotech. Geoenviron. Eng.*, **127**(2), 185-192. [https://doi.org/10.1061/\(ASCE\)1090-0241\(2001\)127:2\(185\)](https://doi.org/10.1061/(ASCE)1090-0241(2001)127:2(185)).
- Morelli, F., Amico, C., Salvatore, W., Squeglia, N. and Stacul, S. (2017), "Influence of tension stiffening on the flexural stiffness of reinforced concrete circular sections", *Materials*, **10**(6), 669. <https://doi.org/10.3390/ma10060669>.
- Nakanishi, K. and Takewaki, I. (2013), "Optimum pile arrangement in piled raft foundation by using simplified settlement analysis and adaptive step-length algorithm", *Geomech. Eng.*, **5**(6), 519-540. <https://doi.org/10.12989/gae.2013.5.6.519>.
- O'Neill, M.W. and Dunnavant, T.W. (1984), "A study of effect of scale, velocity, and cyclic degradability on laterally loaded single piles in overconsolidated clay", University of Houston, Houston, Texas, U.S.A.
- Plaxis BV (2015), *User Manual*, Plaxis 3D Anniversary Edition 2015.
- Poulos, H.G. (1999), "Approximate computer analysis of pile groups subjected to loads and ground movements", *Int. J. Numer. Anal. Meth. Geomech.*, **23**(10), 1021-1041. [https://doi.org/10.1002/\(SICI\)1096-9853\(19990825\)23:10%3C1021::AID-NAG38%3E3.0.CO;2-N](https://doi.org/10.1002/(SICI)1096-9853(19990825)23:10%3C1021::AID-NAG38%3E3.0.CO;2-N).
- Poulos, H.G. (1990), *User's Guide to Program DEFPIG 3/4 Deformation Analysis of Pile Groups*, Revision 6, School of Civil Engineering, University of Sydney, Sydney, Australia.
- Poulos, H.G. (2000), *Practical Design Procedures for Piled Raft Foundations*, in *Design Applications of Raft Foundations*, Thomas Telford, 425-467.
- Poulos, H.G. and Davis, E.H. (1980), *Pile Foundation Analysis and Design*, John Wiley & Sons.
- Press, W., Flannery, B., Teukolsky, S. and Vetterling, W. (1992), *Numerical Recipes in C: The Art of Scientific Computing*, Cambridge University Press.
- Randolph, M.F. (1994), "Design methods for piled groups and piled rafts", *Proceedings of the 13th International Conference of Soil Mechanics and Foundations*, New Delhi, India, January.
- Reese, L.C., Cox, W.R. and Koop, F.D. (1974), "Analysis of laterally loaded piles in sand", *Proceedings of the 6th Annual Offshore Technology Conference*, Houston, Texas, U.S.A., May.
- Reese, L.C., Cox, W.R. and Koop, F.D. (1975), "Field testing and analysis of laterally loaded piles in stiff clay", *Proceedings of the Offshore Technology Conference*, Houston, Texas, U.S.A., May.
- Rollins, K.M., Gerber, T.M., Lane, J.D. and Ashford, S.A. (2005), "Lateral resistance of a full-scale pile group in liquefied sand", *J. Geotech. Geoenviron. Eng.*, **131**(1), 115-125. [https://doi.org/10.1061/\(ASCE\)1090-0241\(2005\)131:1\(115\)](https://doi.org/10.1061/(ASCE)1090-0241(2005)131:1(115)).
- Russo, G. (1998), "Numerical analysis of piled rafts", *Int. J. Numer. Anal. Meth. Geomech.*, **22**(6), 477-493. [https://doi.org/10.1002/\(SICI\)1096-9853\(199806\)22:6%3C477::AID-NAG931%3E3.0.CO;2-H](https://doi.org/10.1002/(SICI)1096-9853(199806)22:6%3C477::AID-NAG931%3E3.0.CO;2-H).
- Russo, G. (2016), "A method to compute the non-linear behaviour of piles under horizontal loading", *Soils Found.*, **56**(1), 33-43. <https://doi.org/10.1016/j.sandf.2016.01.003>.
- Russo, G. (2018), "Analysis and design of pile foundations under

- vertical load: An overview”, *Italian Geotech. J.*, **52**(2), 52-71.
- Russo, G. and Viggiani, C. (2009), “Piles under horizontal load: an overview”, *Proceedings of the 2nd British Geotechnical Association International Conference on Foundations*, Dundee, U.K., June.
- Russo, G., Abagnara, V., Poulos, H.G. and Small, J.C. (2013), “Re-assessment of foundation settlements for the Burj Khalifa, Dubai”, *Acta Geotech.*, **8**(1), 3-15.
<https://doi.org/10.1007/s11440-012-0193-4>.
- Sawada, K. and Takemura, J. (2014), “Centrifuge model tests on piled raft foundation in sand subjected to lateral and moment loads”, *Soils Found.*, **54**(2), 126-140.
<https://doi.org/10.1016/j.sandf.2014.02.005>.
- Sharafkhan, M. and Shooshpasha, I. (2018), “Physical modeling of behaviors of cast-in-place concrete piled raft compared to free-standing pile group in sand”, *J. Rock Mech. Geotech. Eng.*, **10**(4), 703-716. <https://doi.org/10.1016/j.jrmge.2017.12.007>.
- Small, J.C. and Booker, J.R. (1986), “Finite layer analysis of layered elastic materials using a flexibility approach. Part 2—Circular and rectangular loadings”, *Int. J. Numer. Meth. Eng.*, **23**(5), 959-978. <https://doi.org/10.1002/nme.1620230515>.
- Small, J.C. and Zhang, H.H. (2000), “Piled raft foundations subjected to general loadings”, *Dev. Theor. Geomech.*, 431-444.
- Small, J.C. and Zhang, H.H. (2002), “Behavior of piled raft foundations under lateral and vertical loading”, *Int. J. Geomech.*, **2**(1), 29-45.
[https://doi.org/10.1061/\(ASCE\)1532-3641\(2002\)2:1\(29\)](https://doi.org/10.1061/(ASCE)1532-3641(2002)2:1(29)).
- Small, J.C., Zhang, H.H. and de Ambrosis, A.L. (2006), “Analysis of piled raft foundation”, Department of Civil Engineering, University of New South Wales Sydney, Sydney, Australia.
- Stacul, S. (2018), “Analysis of piles and piled raft foundation under horizontal load”, Ph.D. Dissertation, University of Florence, Florence, Italy, Technical University of Braunschweig, Braunschweig, Germany.
- Stacul, S. and Squeglia, N. (2018), “Analysis method for laterally loaded pile groups using an advanced modeling of reinforced concrete sections”, *Materials*, **11**(2), 300.
<https://doi.org/10.3390/ma11020300>.
- Stacul, S., Squeglia, N. and Morelli, F. (2017), “Laterally loaded single pile response considering the influence of suction and non-linear behaviour of reinforced concrete sections”, *Appl. Sci.*, **7**(12), 1310. <https://doi.org/10.3390/app7121310>.
- Unsever, Y., Ozkan, M., Matsumoto, T., Shimono, S. and Esashi, K. (2014), “Physical and numerical modelling of pile foundations subjected to vertical and horizontal loading in dry sand”, *Proceedings of the 14th International Conference of International Association for Computer Methods and Recent Advances in Geomechanics, 2014 (IACMAG 2014)*, Kyoto, Japan, September.
- Unsever, Y.S., Matsumoto, T. and Özkan, M.Y. (2015), “Numerical analyses of load tests on model foundations in dry sand”, *Comput. Geotech.*, **63**, 255-266.
<https://doi.org/10.1016/j.compgeo.2014.10.005>.
- Viggiani, C., Mandolini, A. and Russo, G. (2012), *Piles and Pile Foundations*, Spoon Press.
- Vu, A.T., Matsumoto, T., Kobayashi, S.I. and Nguyen, T.L. (2016), “Model load tests on battered pile foundations and finite-element analysis”, *Int. J. Phys. Modell. Geotech.*, **18**(1), 33-54.
<https://doi.org/10.1680/jphmg.16.00010>.
- Vu, A.T., Matsumoto, T., Kobayashi, S.I. and Shimono, S. (2017), “Experimental study on pile foundations having batter piles subjected to combination of vertical and horizontal loading at 1-g field”, *Geotech. Eng. J. SEAGS AGSSEA*, **48**(3), 12-24.
- Welch, R.C. and Reese, L.C. (1972), “Lateral load behavior of drilled shafts”, Research Report No. 89-10, University of Texas at Austin, Austin, Texas, U.S.A.
- Wu, G., Liam Finn, W.D. and Dowling, J. (2015), “Quasi-3D analysis: validation by full 3D analysis and field tests on single piles and pile groups”, *Soil Dyn. Earthq. Eng.*, **78**, 61-70.
<https://doi.org/10.1016/j.soildyn.2015.07.006>.
- Yang, Z. and Jeremic, B. (2002), “Numerical analysis of pile behaviour under lateral loads in layered elastic-plastic soils”, *Int. J. Numer. Anal. Meth. Geomech.*, **26**(14), 1385-1406.
<https://doi.org/10.1002/nag.250>.
- Yang, Z. and Jeremic, B. (2003), “Numerical study of group effects for pile groups in sands”, *Int. J. Numer. Anal. Meth. Geomech.*, **27**(15), 1255-1276. <https://doi.org/10.1002/nag.321>.
- Zhang, H.H. and Small, J.C. (2000), “Analysis of capped pile groups subjected to horizontal and vertical loads”, *Comput. Geotech.*, **26**, 1-21.
[https://doi.org/10.1016/S0266-352X\(99\)00029-4](https://doi.org/10.1016/S0266-352X(99)00029-4).

CC